GSVD Beamforming for Two-User MIMO Downlink Channel

Damith Senaratne, *Member, IEEE*, and Chintha Tellambura, *Fellow, IEEE*

Abstract—This paper introduces the fundamentals of generalized singular value decomposition (GSVD) beamforming: a noniterative beamforming technique based on GSVD for the two-user multiple-input–multiple-output (MIMO) downlink. The numbers of private/common channels produced by GSVD beamforming and transmit power normalization are investigated; the channel gains under Rayleigh fading are characterized exactly for configurations that involve only common channels. Moreover, symbol error rates (SERs) are presented for elementary multicasting and two-way relaying applications; the performance distinctions of the private/common channels and the effect of channel-estimation errors and asymmetries in channel fading are highlighted thereby.

Index Terms—Beamforming, generalized singular value decomposition (GSVD), multicasting, network-coded two-way relaying, β-Jacobi ensemble.

I. INTRODUCTION

WITH the ever-increasing end-user demand for wireless multimedia content, *multicasting*, i.e., point-to-multipoint delivery of data, has become a core capability of wireless networks. For example, the IEEE 802.11-2012 standard [1], which is the latest revision of Wi-Fi, as well as the evolved multimedia broadcast multicast services [2] specification for the Third-Generation Partnership Project Long-Term Evolution (3GPP LTE) and LTE-Advanced standards, supports multicasting. Apart from multicasting, relaying applications also call for point-to-multipoint delivery of data.

To support multicasting, multiple logical channels, which are also known as virtual channels (VCs), are implemented over the physical wireless channel. Beamforming enables these VCs, facilitating the deployment of the modulation, coding, and resource allocation techniques for single-antenna systems in multiple-input–multiple-output (MIMO) systems. However, point-to-multipoint data delivery is not well supported by conventional beamforming techniques such as zero forcing (ZF) and block diagonalization [3], which are designed to produce multiple point-to-point VCs. Such techniques must repeat the same data over multiple VCs to realize multicasting and, therefore, underutilize the spatial degrees of freedom (DoFs). Physical-layer multicasting (PLM) [4] addresses this

The authors are with the Department of Electrical and Computer Engineering, University of Alberta, Edmonton, AB T6G 2V4, Canada (e-mail: damith@ieee.org; chintha@ece.ualberta.ca).
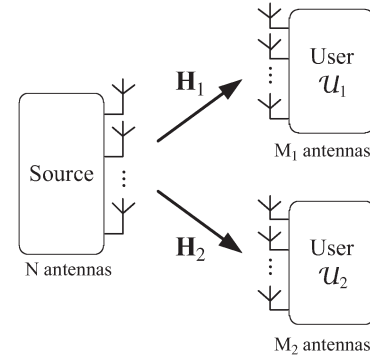
Fig. 1.　Two-user MIMO downlink configuration.

issue by jointly computing the transmit beamforming matrix and the receiver beamforming matrices to realize point-to-multipoint VCs. However, the computations in PLM [5]–[9] are iterative and with high computational complexity. Thus, developing noniterative beamforming alternatives for multiuser MIMO channels is of great interest.

GSVD beamforming [10] is such a noniterative beamforming technique for two-user MIMO channels (see Fig. 1). It is based on the generalized singular value decomposition (GSVD) [11], a technique for joint diagonalization of two matrices. Basically, the GSVD computes a rightmost factor common to two matrices so that the singular value decompositions (SVDs) [12, p. 142] of their remainders have the same right singular vectors. In GSVD beamforming, transmit processing inverts the common factor and right singular vectors; receiver processing is based on the left singular vectors given by those SVDs. Therefore, while generalizing the SVD for the two-user downlink, GSVD beamforming also generalizes *transmit* ZF.[1]

Despite being limited to two users, GSVD beamforming yields common channels (CCs), i.e., point-to-two point VCs that cater to both the users, in addition to private channels (PCs), the classic point-to-point VCs that cater to individual users. Thus, GSVD beamforming can meet the end-user requirements for multicasting by implementing the desired combination of CCs and PCs. For the system in Fig. 1, GSVD can split the two-user MIMO channel into PCs and CCs, where each PC is a VC from $\mathcal{S}$ to $\mathcal{U}_1$ (or $\mathcal{U}_2$), and each CC is a VC from $\mathcal{S}$ to $\mathcal{U}_1$ and $\mathcal{U}_2$ simultaneously. GSVD beamforming holds, irrespective of the spatial DoFs available at the terminals and the rank-deficiencies of the channels; however, to maximally exploit DoFs at all three terminals, the numbers of PCs and CCs

---

[1]In fact, GSVD beamforming reduces to transmit ZF when the source has more antennas than the two users combined.

realized vary with the system configuration. These facts make GSVD beamforming worth investigating.

Being a natural generalization of the well-known SVD, the GSVD has been used in different wireless applications, for example, in MIMO secrecy communication [13], [14] and MIMO relaying [15]. However, it has not been exploited for beamforming until [10], despite its beamforming potential being mentioned in [13, p. 1]. Although GSVD is related to the generalized eigenvalue decomposition (for square matrices), GSVD beamforing is semantically different from generalized eigenvector-based beamforming techniques [16], [17]. Therefore, insights into GSVD beamforming are wanting in the literature. This paper investigates GSVD beamforming to further our understanding of the corresponding VC gains and the symbol-error-rate (SER) performance of its applications.

The contributions of this paper are listed as follows.

- For a system with only CCs, the joint distribution of the gains and their diversity orders are derived, assuming independent and identically distributed (i.i.d.) Rayleigh fading. These results establish a framework for the exact performance analysis of such systems.
- The dependence of the numbers of PCs and CCs on the channel ranks is investigated.
- The SERs for a simple two-user multicast application are simulated to investigate the relative performance differences in the PCs and CCs, as well as the effects of channel-estimation errors and the asymmetries.
- In network-coded two-way relaying, similar to Fig. 1, the relay communicates with two users, making GSVD beamforming possible. Such a system is investigated with transmit ZF employed in the uplink and GSVD beamforming in the downlink. The corresponding error performance is compared with the performance of beamforming schemes using either ZF or GSVD for both the uplink and the downlink.

This paper is organized as follows. Section II introduces GSVD, highlighting how GSVD-based signal processing realizes the PCs and CCs. Section III, for systems with only CCs, derives the exact joint probability density function (pdf) of the gains under i.i.d. Rayleigh fading. The dependence of the numbers of PCs/CCs on the spatial DoFs is examined in Section IV, whereas Section V discusses transmit power normalization. Numerical results on the SER, including results on elementary multicasting and two-way relaying applications, are presented in Section VI. The conclusion follows in Section VII, and the proof of Theorem 1 is annexed in the Appendix.

A. Notation

$\mathbf{A} \in \mathbb{C}^{m \times n}$ is an $m \times n$ complex matrix. Its conjugate, transpose, conjugate transpose, Moore–Penrose pseudoinverse, rank, and Frobenius norm are given by $\mathbf{A}^*$, $\mathbf{A}^T$, $\mathbf{A}^H$, $\mathbf{A}^{\dagger}$, rank $(\mathbf{A})$, and $\|\mathbf{A}\|_F$, respectively. $\{\mathbf{A}\}_{\mathcal{R}(m_1;m_2)}$, $\{\mathbf{A}\}_{\mathcal{C}(n_1;n_2)}$, and $\{\mathbf{A}\}_{\mathcal{C}(\mathcal{L})}$ denote, respectively, the submatrices of $\mathbf{A}$ formed with its rows m_1–m_2, columns n_1–n_2, and columns whose indices are in set $\mathcal{L} \subseteq \{1, \dots, n\}$. $\mathbf{B} = \text{diag}(b_1, \dots, b_p)$ is a (rectangular) diagonal matrix, and $\text{diag}(\mathbf{B})$ are the main diagonal elements b_1–b_p. For $\mathbf{C} \in \mathbb{C}^{n \times n}$, $\text{eig}(\mathbf{C})$, $\mathbf{C}^{-1}$, and trace $(\mathbf{C})$ represent the eigenvalues, the inverse, and the trace of $\mathbf{C}$. $\mathcal{E}\{X\}$ denotes the expectation, whereas $\mathcal{O}(\cdot)$ is the big O notation.

II. Generalized Singular Value Decomposition Signal Processing

In the literature, GSVD is found in the following two forms: 1) the original definition by Van Loan [11, Th. 2] (Definition 1) and 2) a generalization by Paige and Saunders [18] (Definition 2). Each form is given as follows, highlighting how its characteristics pertain to GSVD beamforming.

Definition 1: Van Loan Form: Consider two matrices $\mathbf{H}_1 \in \mathbb{C}^{m \times n}$ with $m \geq n$ and $\mathbf{H}_2 \in \mathbb{C}^{p \times n}$, which have the same number n of columns. Let $q = \min(p, n)$. $\mathbf{H}_1$ and $\mathbf{H}_2$ can jointly be decomposed as

$$\mathbf{H}_1 = \mathbf{U}\mathbf{\Sigma}\mathbf{Q} \text{ and } \mathbf{H}_2 = \mathbf{V}\mathbf{\Lambda}\mathbf{Q} \tag{1}$$

where the following conditions hold.

1. $\mathbf{U} \in \mathbb{C}^{m \times m}$ and $\mathbf{V} \in \mathbb{C}^{p \times p}$ are unitary.
2. $\mathbf{Q} \in \mathbb{C}^{n \times n}$ is nonsingular.
3. $\mathbf{\Sigma} = \text{diag}(\sigma_1, \dots, \sigma_n) \in \mathbb{C}^{m \times n}$, $\sigma_i \geq 0$, and $\mathbf{\Lambda} = \text{diag}(\lambda_1, \dots, \lambda_q) \in \mathbb{C}^{p \times n}$, $\lambda_i \geq 0$
●

Suppose that $\mathbf{H}_1$ and $\mathbf{H}_2$ in (1) represent MIMO channels $\mathcal{S} \to \mathcal{U}_1$ and $\mathcal{S} \to \mathcal{U}_2$ from a source $\mathcal{S}$ to users $\mathcal{U}_1$ and $\mathcal{U}_2$. Assume block fading and perfect channel-state information (CSI) on $\mathbf{H}_1$ and $\mathbf{H}_2$ at all $\mathcal{S}, \mathcal{U}_1$, and $\mathcal{U}_2$. With a transmit precoding matrix $\rho\mathbf{Q}^{-1}$ and receiver reconstruction matrices $\mathbf{U}^H/\rho$ and $\mathbf{V}^H/\rho$, we get q noninterfering broadcast VCs, each catering to both users. The factor $\mathbf{Q}$ in (1) facilitates joint precoding, whereas the factors $\mathbf{U}$ and $\mathbf{V}$ enable receiver reconstruction without noise enhancement. The diagonal elements of $\mathbf{\Sigma}$ and $\mathbf{\Lambda}$ represent the gains of those VCs. Because $\mathbf{Q}$ is nonunitary, precoding causes the instantaneous transmit power to fluctuate; this result is a drawback, and a transmit signal needs to be normalized to maintain the desired level of average transmit power. (The coefficient ρ represents transmit power normalization.) Thus, GSVD beamforming is applicable for two-user channels. Because this three-terminal configuration appears in various MIMO subsystems, GSVD beamforming has the potential to be a useful tool.

Definition 2: Paige and Saunders Form: Consider matrices $\mathbf{H}_1 \in \mathbb{C}^{m \times n}$ and $\mathbf{H}_2 \in \mathbb{C}^{p \times n}$, which have the same number n of columns. Let $\mathbf{H}_0 = (\mathbf{H}_1^T, \mathbf{H}_2^T)^T$, $k = \text{rank}(\mathbf{H}_0)$, $r = k - \text{rank}(\mathbf{H}_2)$, and $s = \text{rank}(\mathbf{H}_1) + \text{rank}(\mathbf{H}_2) - k$. Unitary matrices $\mathbf{U} \in \mathbb{C}^{m \times m}$, $\mathbf{V} \in \mathbb{C}^{p \times p}$, $\mathbf{W} \in \mathbb{C}^{k \times k}$, and $\mathbf{Q} \in \mathbb{C}^{n \times n}$ can be found such that

$$\mathbf{H}_1 = \mathbf{U} \cdot \mathbf{\Sigma}_1 \cdot (\mathbf{W}^H \mathbf{R}, \mathbf{0})\mathbf{Q}^H \text{ and}$$
$$\mathbf{H}_2 = \mathbf{V} \cdot \mathbf{\Sigma}_2 \cdot (\mathbf{W}^H \mathbf{R}, \mathbf{0})\mathbf{Q}^H \tag{2}$$

where the following conditions hold.

1. $\mathbf{\Sigma}_1 \in \mathbb{C}^{m \times k}$, $\mathbf{\Sigma}_2 \in \mathbb{C}^{p \times k}$ have block-diagonal structures, i.e.,

$$\mathbf{\Sigma}_1 \triangleq \begin{pmatrix} \mathbf{I}_1 & & \\ & \mathbf{S}_1 & \\ & & \mathbf{0}_1 \end{pmatrix} \text{ and } \mathbf{\Sigma}_2 \triangleq \begin{pmatrix} \mathbf{0}_2 & & \\ & \mathbf{S}_2 & \\ & & \mathbf{I}_2 \end{pmatrix}. \tag{3}$$

2. $\mathbf{R} \in \mathbb{C}^{k \times k}$ is invertible and has the same singular values as the nonzero singular values of $\mathbf{H}_0$.
3. $\mathbf{0} \in \mathbb{C}^{k \times (n-k)}$ is a zero matrix.
4. $\mathbf{I}_1 \in \mathbb{C}^{r \times r}$ and $\mathbf{I}_2 \in \mathbb{C}^{(k-r-s) \times (k-r-s)}$ are identity matrices.
5. $\mathbf{0}_1 \in \mathbb{C}^{(m-r-s) \times (k-r-s)}$ and $\mathbf{0}_2 \in \mathbb{C}^{(p-k+r) \times r}$ are zero matrices that possibly have no rows or no columns.
6. $\mathbf{S}_1 = \mathrm{diag}\ (\alpha_1, \ldots, \alpha_s)$ and $\mathbf{S}_2 = \mathrm{diag}\ (\beta_1, \ldots, \beta_s)$ such that $1 > \alpha_1 \geq \ldots \geq \alpha_s > 0$ and $\alpha_i^2 + \beta_i^2 = 1$ for $i \in \{1, \ldots, s\}$.   •

If matrices $\mathbf{H}_1$ and $\mathbf{H}_2$ represent wireless channels that correspond to $\mathcal{S} \rightarrow \mathcal{U}_1$ and $\mathcal{S} \rightarrow \mathcal{U}_2$ as aforementioned, the beamforming matrices $\rho\{\mathbf{Q}\}_{\mathcal{C}(1:k)}\mathbf{R}^{-1}\mathbf{W}$ at the source and $\mathbf{U}^H/\rho$, $\mathbf{V}^H/\rho$ at the respective users $\mathcal{U}_1$, $\mathcal{U}_2$ reduce the effective channels between the source and the users to $\mathbf{\Sigma}_1$ and $\mathbf{\Sigma}_2$, respectively.

Each column of $\mathbf{\Sigma}_1$ (and $\mathbf{\Sigma}_2$) corresponds to a VC (either a PC or a CC) from the source. The following conditions hold.

- The sets of columns $\{1, \ldots, r\}$ and $\{r + s + 1, \ldots, k\}$, if nonempty, produce, respectively, r and $(k - r - s)$ PCs for $\mathcal{U}_1$ and $\mathcal{U}_2$, each PC catering to just one user and having a unit gain.
- The columns $\{r + 1, \ldots, r + s\}$ that correspond to $\mathbf{S}_1$ (and $\mathbf{S}_2$) yield s point-to-two point CCs. The corresponding amplitude gains experienced by $\mathcal{U}_1$ are given by α_i for $i \in \{1, \ldots, s\}$. Likewise, the β_i's represent the gains experienced by $\mathcal{U}_2$.

Any subset of VCs may be selected by appropriately leaving out certain columns from the transmit beamforming matrix and the corresponding rows from the receiver beamforming matrices. When $(\mathbf{H}_0) = \mathrm{rank}\ (\mathbf{H}_1) + \mathrm{rank}\ (\mathbf{H}_2)$, s becomes zero, and the scheme reduces to transmit ZF. This process is the essence of GSVD beamforming as a tool for multiplexing private and/or common data streams that cater to two users.

Not only is Definition 2 more general than Definition 1 but it also makes the GSVD of two matrices unique. (Reference [18] outlines the decomposition step by step.) The GSVD of matrices $\mathbf{H}_1 \in \mathbb{C}^{m \times n}$ and $\mathbf{H}_2 \in \mathbb{C}^{p \times n}$ requires the SVD of the $(m + p) \times n$ matrix $\mathbf{H}_0 = (\mathbf{H}_1^T, \mathbf{H}_2^T)^T$, followed by the SVD of an $m \times k$ matrix, the QR decomposition [12, p. 131] of a $p \times k$ matrix, and several intermediate matrix multiplications, where $k = \mathrm{rank}\ (\mathbf{H}_0)$. Hence, its computational complexity is $\mathcal{O}((m + p) \cdot n \times \min(m + p, n))$, which is of the same order as that of computing the SVD of $\mathbf{H}_0$, the effective channel seen by the source $\mathcal{S}$. This observation also indicates that iterative beamforming schemes are likely to have similar complexity per iteration.

III. CHARACTERIZATION OF CHANNEL GAINS

As outlined in Section II, the GSVD of channel matrices $\mathbf{H}_1 \in \mathbb{C}^{m \times n}$ and $\mathbf{H}_2 \in \mathbb{C}^{p \times n}$, corresponding to users $\mathcal{U}_1$ and $\mathcal{U}_2$, is of the form $\mathbf{H}_1 = \mathbf{U}\mathbf{\Sigma}_1 (\mathbf{W}^H\mathbf{R}, \mathbf{0})\ \mathbf{Q}^H$ and $\mathbf{H}_2 = \mathbf{V}\mathbf{\Sigma}_2 (\mathbf{W}^H\mathbf{R}, \mathbf{0})\ \mathbf{Q}^H$. All PCs have unit gains. The gain experienced for each ith CC CC_i by $\mathcal{U}_1$ is given by $\alpha_i \in \mathrm{diag}\ (\mathbf{\Sigma}_1), \alpha_i \in (0, 1)$, a distinct nontrivial diagonal element of $\mathbf{\Sigma}_1$ for $i \in \{1, \ldots, s\}$. Because $\beta_i = \sqrt{1 - \alpha_i^2}$, each α_i also characterizes the gain experienced by $\mathcal{U}_2$ for CC_i.

Let $\mathbf{P} \in \mathbb{C}^{(m+p) \times (m+p)}$ be the matrix formed with the left singular vectors of $\mathbf{H}_0 = (\mathbf{H}_1^T, \mathbf{H}_2^T)^T$ and $k = \mathrm{rank}\ (\mathbf{H}_0)$. The α_i's are nontrivial singular values of the $m \times k$ submatrix $\mathbf{Q} = \{\{\mathbf{P}\}_{\mathcal{C}(1;k)}\}_{\mathcal{R}(1:m)}$, the trivial ones being 0 or 1 [18, eq. (2.7)]; thus, we have $\{\alpha_i | \alpha_i^2 \in \mathrm{eig}\ (\mathbf{Q}^H\ \mathbf{Q}) - \{0, 1\}\}$. The eigenvalue distribution of $\mathbf{Q}^H\ \mathbf{Q}$ is not known in general. However, it can be found under certain rank restrictions when $\mathbf{P}$ is a Haar-distributed random unitary matrix [19, Sec. 2.1.4]. This scenario corresponds to $\mathbf{H}_1$ and $\mathbf{H}_2$ undergoing i.i.d. Rayleigh fading, because the singular vectors of a complex Gaussian matrix produce a Haar-distributed random unitary matrix when concatenated. The eigenvalue distribution depends only on the ranks of $\mathbf{H}_1$, $\mathbf{H}_2$, and $\mathbf{H}_0$ or, in other words, on the spatial DoFs available at $\mathcal{U}_1$, $\mathcal{U}_2$, and the source. This observation is not surprising, because the factor $\mathbf{R}^{-1}\ \mathbf{W}$ of the transmit precoding matrix effectively inverts $\mathbf{H}_0$, the MIMO channel the source has with the users. This inversion is also the reason that GSVD beamforming reduces to transmit ZF, where the source has more antennas than the users combined.

The eigenvalue distribution of $v \times v$ (square) truncations of $(u + v) \times (u + v)$ Haar-distributed unitary matrices has been examined in the literature [20], [21] for the case $v < u$; however, the results are not general enough to characterize GSVD beamforming. The eigenvalue distribution of the β-*Jacobi ensemble* [22, Ch. 5] is more relevant, because whenever $m \geq k$ and $p \geq k$, the squared α_i's follow the same joint distribution as the eigenvalues of the β-Jacobi ensemble [23, Prop. 1.2] for $\beta = 2$. Applying the variable transformation $\lambda_i = \alpha_i^2$ on the joint pdf [24, eq. (5)] of the ordered eigenvalues λ_i's of the β-Jacobi ensemble (for $\beta = 2$), we get Proposition 1. Note that the condition $\min (m, p) \geq k$ restricts it to configurations that support only CCs (with $k \doteq s$).

Proposition 1: Where $\min (m, p) \geq k$, the joint pdf of the ordered α_i's, $\alpha_i \in \mathrm{diag}\ (\mathbf{\Sigma}_1)$ for $\mathbf{\Sigma}_1$ in (3), is given by

$$f_\alpha(\alpha_1, \ldots \alpha_k) = c_{m,p,k} \prod_{i=1}^{k} \alpha_i^{2(m-k)+1}(1 - \alpha_i^2)^{p-k}$$

$$\times \prod_{I \leq i \leq j \leq k} (\alpha_i^2 - \alpha_j^2) \quad (4)$$

for $1 > \alpha_1 > \ldots > \alpha_k > 0$, where

$$c_{m,p,k} = k! \cdot 2^k \prod_{i=1}^{k} \frac{(m + p - i)}{i!(m - i)!(p - i)}. \quad (5)$$

   •

The joint pdf of the unordered α_i's has the same expression as in (4), except for the factor $k!$ in (5).

Fig. 2 compares, for the case $(m, p, k) \doteq (2, 5, 2)$, the joint pdf of α_1 and α_2 analytically obtained by using Proposition 1 against 10^8-point Monte Carlo simulation results. The figure reveals the exact agreement of the analytical and simulation results, which also conform with the fact that $\alpha_i \in (0, 1)$. Proposition 1 can be used for the performance analysis of configurations that support only CCs; Theorem 1 on the diversity orders exemplifies the proposition's usefulness.
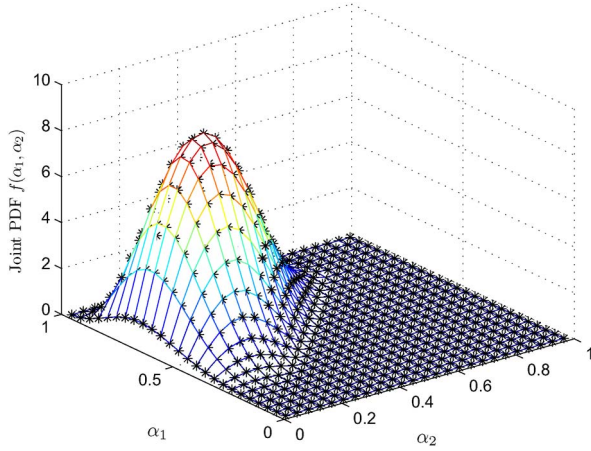
Fig. 2. Joint pdf of α_i's in Definition 2 for $(m, p, k) \doteq (2, 5, 2)$—analytic based on (4) versus the simulated $*$.
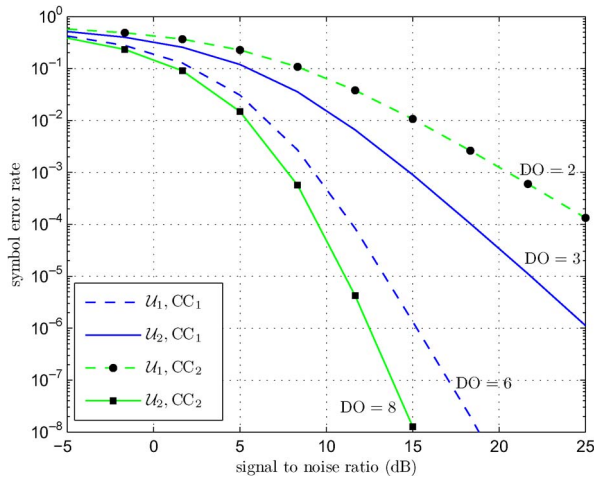

Fig. 3. SERs and diversity orders of the CCs in the $(N, M_1, M_2) \doteq (2, 3, 4)$ two-user downlink configuration. The gradients of the SER curves at a high SNR correspond to the diversity orders DO = $\{2, 3, 6, 8\}$. QPSK modulation is used.

Theorem 1: Diversity Order for the Case $\min (m, p) \geq k$: Consider GSVD beamforming over MIMO channels $\mathbf{H}_1 \in \mathbb{C}^{m \times n}$ and $\mathbf{H}_2 \in \mathbb{C}^{p \times n}$, corresponding to users $\mathcal{U}_1$ and $\mathcal{U}_2$ undergoing i.i.d. Rayleigh fading. Suppose rank $((\mathbf{H}_1^T, \mathbf{H}_2^T)) = k \leq \min (m, p)$. Then, the diversity order of CC_r for $\mathcal{U}_1$ is given by $(m - r + 1)(k - r + 1)$ for $r \in \{1, \dots, k\}$. •

Proof: See the Appendix. ■

The diversity orders $(m - r + 1)(k - r + 1)$ for CC_r, $r \in \{1, \dots, k\}$ are intuitive, because the α_r's are the sorted singular values of an $m \times k$ matrix. In fact, the diversity orders are the same as those corresponding to eigenmode transmission between the source and $\mathcal{U}_1$ (or $\mathcal{U}_2$) alone. For $r > k$, they exceed $(m - k + 1)$, which is the diversity order of the CCs that ZF reception provides. For an $(N, M_1, M_2) \doteq (2, 3, 4)$-antenna two-user multicast configuration that involves users $\mathcal{U}_1$ and $\mathcal{U}_2$ and corresponds to $k = 2$, $m = 4$, and $p = 4$, Fig. 3 verifies that GSVD beamforming yields a diversity order of $(3 - r + 1) \times (2 - r + 1)$ for each CC_r, $r \in \{1, 2\}$ of $\mathcal{U}_1$. Likewise, a diversity order $(4 - (3 - r) + 1) \times (2 - (3 - r) + 1)$ is observed for each CC_r of $\mathcal{U}_2$. 10^8-point Monte Carlo simulation with 100 quadrature phase-shift keying (QPSK)-

TABLE I
NUMBERS OF CCs AND PCs REALIZED THROUGH GSVD BEAMFORMING FOR ANTENNAS (n, m, p) AT THE SOURCE AND USERS $\mathcal{U}_1, \mathcal{U}_2$, RESPECTIVELY

| configuration | # CCs | # PCs | |
	$S \rightarrow \{\mathcal{U}_1, \mathcal{U}_2\}$	$S \rightarrow \mathcal{U}_1$	$S \rightarrow \mathcal{U}_2$
$m > n, p \leq n$	p	$n - p$	0
$m \leq n, p > n$	m	0	$n - m$
$m \geq n, p \geq n$	n	0	0
$m < n, p < n,$ $(m + p) > n$	$m + p - n$	$n - p$	$n - m$
$n \geq (m + p)$	0	m	p

modulated symbols per VC per channel realization is used to obtain the SER curves.

Numerical analysis based on (4) is inherently simple, given the finite range $(0, 1)$ of α_i, $i \in \{1, \dots, k\}$. Because standard integral expressions used in wireless performance analysis typically assume a $[0, \infty)$ range, the finite range could, however, complicate most exact analyses.

IV. NUMBERS OF PRIVATE CHANNELS/COMMON CHANNELS

As outlined in Section II, GSVD beamforming on the channels $\mathbf{H}_1 \in \mathbb{C}^{m \times n}$ and $\mathbf{H}_2 \in \mathbb{C}^{p \times n}$ that correspond to users $\mathcal{U}_1$ and $\mathcal{U}_2$ yields s CCs, r PCs for $\mathcal{U}_1$, and $(k - r - s)$ PCs for $\mathcal{U}_2$. The numbers of VCs add up to $k = \mathrm{rank} (\mathbf{H}_0)$, indicating full utilization of the spatial DoFs at the source for multiplexing.

The numbers $k = \mathrm{rank} (\mathbf{H}_0)$, $r = k - \mathrm{rank} (\mathbf{H}_2)$, and $s = \mathrm{rank} (\mathbf{H}_1) + \mathrm{rank} (\mathbf{H}_2) - k$ are governed by the MIMO channel ranks. Where the channels are not rank deficient as with rich scattering, $k = \min (m + p, n)$, $r = k - \min (p, n)$, and $s = \min (m, n) + \min (p, n) - k$ depend on the number of antennas at the three terminals. Consequently, the numbers of VCs are fixed, given an antenna configuration (see Table I). The ensuing lack of flexibility can be circumvented by using additional transmit and/or receiver processing[2] for rank reduction, i.e., by reducing the *effective* number of antennas, as highlighted in Example 1.

Example 1: Let $\tilde{m} = n_c + n_{p_1} \leq m$, $\tilde{p} = n_c + n_{p_2} \leq p$, and $\tilde{n} = n_c + n_{p_1} + n_{p_2} \leq n$ be the effective numbers of antennas required, respectively, at users $\mathcal{U}_1$ and $\mathcal{U}_2$ and the source to realize the desired numbers of VCs, i.e., n_c CCs and n_{p_1}, n_{p_2} PCs that cater to $\mathcal{U}_1, \mathcal{U}_2$. These numbers are achievable as follows, provided that $k = \mathrm{rank} (\mathbf{H}_0) \geq \tilde{n}$.

Suppose that $\mathbf{H}_1 = \mathbf{U}_1 \mathbf{\Lambda}_1 \mathbf{V}_1^H$, $\mathbf{H}_2 = \mathbf{U}_2 \mathbf{\Lambda}_2 \mathbf{V}_2^H$, and $\mathbf{H}_0 = (\mathbf{H}_1^T, \mathbf{H}_2^T)^T = \mathbf{U}_0 \mathbf{\Lambda}_0 \mathbf{V}_0^H$ are the SVDs. Define $\mathbf{X}_1 = \{\mathbf{U}_1^H\}_{\mathcal{R}(1;\tilde{m})}, \mathbf{X}_2 = \{\mathbf{U}_2^H\}_{\mathcal{R}(1;\tilde{p})}$, and $\mathbf{X}_0 = \{\mathbf{V}_0\}_{\mathcal{C}(1;\tilde{n})}$. Then, compute the GSVD as follows:

$$\mathbf{X}_1 \mathbf{H}_1 \mathbf{X}_0 = \mathbf{U} \cdot \mathbf{\Sigma}_1 \cdot (\mathbf{W}^H \mathbf{R}, \mathbf{0}) \mathbf{Q}^H \text{ and}$$

$$\mathbf{X}_2 \mathbf{H}_2 \mathbf{X}_0 = \mathbf{V} \cdot \mathbf{\Sigma}_2 \cdot (\mathbf{W}^H \mathbf{R}, \mathbf{0}) \mathbf{Q}^H. \quad (6)$$

The beamforming matrices $\rho \mathbf{X}_0 \{\mathbf{Q}\}_{\mathcal{C}(1:k)} \mathbf{R}^{-1} \mathbf{W}$ at the source, and $\mathbf{U}^H \mathbf{X}_1 / \rho$ and $\mathbf{V}^H \mathbf{X}_2 / \rho$, respectively, at users $\mathcal{U}_1$ and $\mathcal{U}_2$, yield the desired numbers of VCs. Note that the

---

[2]Antenna selection is a less attractive alternative.

products $\mathbf{X}_1\mathbf{H}_1\mathbf{X}_0$ and $\mathbf{X}_2\mathbf{H}_2\mathbf{X}_0$ in (6), acting as the effective matrices for the GSVD, are of reduced dimensions compared with the original matrices $\mathbf{H}_1$ and $\mathbf{H}_2$.   •

V. TRANSMIT POWER NORMALIZATION

Suppose that the transmitted data vector $\mathbf{x} \in \mathbb{C}^{|\mathcal{L}| \times 1}$ is mapped to an arbitrary combination of $|\mathcal{L}|$ PCs/CCs, whose channel gains are represented by the columns of $\mathbf{\Sigma}_1$ and $\mathbf{\Sigma}_2$ that correspond to indices in the set $\mathcal{L} \subseteq \{1, \ldots, k\}$. Such mapping can be realized with a transmit beamforming matrix $\rho\{\mathbf{Q}\}_{\mathcal{C}(1;k)} \mathbf{R}^{-1} \{\mathbf{W}\}_{\mathcal{C}(\mathcal{L})}$, where ρ is the transmit power normalization coefficient that ensures a desired average total transmit power P. Thus, we have

$$P = \rho^2 \mathcal{E} \left\{ \| \{\mathbf{Q}\}_{\mathcal{C}(1;k)} \mathbf{R}^{-1} \{\mathbf{W}\}_{\mathcal{C}(\mathcal{L})} \mathbf{x} \|_F^2 \right\}. \tag{7}$$

Generally, ρ needs to numerically be computed. Nevertheless, it may exactly be derived as follows for special cases.

Assume uncorrelated data and equal energy modulation. Without loss of generality, we may set $\mathcal{E}_{\mathbf{x}}\{\mathbf{x}\mathbf{x}^H\} = \mathbf{I}$ to obtain

$$P = \rho^2 \mathcal{E} \left\{ \text{trace} \left\{ \{\mathbf{W}\}_{\mathcal{C}(\mathcal{L})}^H \mathbf{R}^{-1} \{\mathbf{Q}^H\}_{\mathcal{R}(1:k)} \right. \right.$$
$$\left. \left. \cdot \{\mathbf{W}\}_{\mathcal{C}(1:k)} \mathbf{R}^{-1} \{\mathbf{W}\}_{\mathcal{C}(\mathcal{L})} \right\} \right\}$$
$$= \rho^2 \mathcal{E} \left\{ \text{trace} \left(\mathbf{R}^{-2} \{\mathbf{W}\}_{\mathcal{C}(\mathcal{L})} \{\mathbf{W}\}_{\mathcal{C}(\mathcal{L})}^H \right) \right\}. \tag{8}$$

The product $\{\mathbf{W}\}_{\mathcal{C}(\mathcal{L})} \{\mathbf{W}\}_{\mathcal{C}(\mathcal{L})}^H$ is an identity matrix when $\mathcal{L} \equiv \{1, \ldots, k\}$, i.e., when all the VCs are in use. For that case only and by using the fact that the squared singular values of $\mathbf{R}$ are the nonzero eigenvalues of the $\mathbf{H}_0\mathbf{H}_0^H$ product, we get a simplified expression, i.e.,

$$\rho = \sqrt{\frac{P}{\mathcal{E}\{\text{trace}(\mathbf{R}^{-2})\}}} = \sqrt{\frac{P}{\mathcal{E}\{\sum_{i=1}^k \lambda_i^{-1}\}}} \tag{9}$$

where $\lambda_i \in \text{eig}\left(\mathbf{H}_0\mathbf{H}_0^H\right)$ for $i \in \{1, \ldots, k\}$. By using [19, Lemma 2.10], (9) may further be simplified; for example, $\rho = \sqrt{P|m + p - n|/\min(m + p, n)}$ for i.i.d. Rayleigh fading.

VI. NUMERICAL RESULTS

This section uses the Monte Carlo simulation of the SER to gain insights into how a system performs under GSVD beamforming. A two-user MIMO multicast configuration is considered first, and a network-coded two-way relay configuration is investigated next.

Assumptions: Block fading is assumed, and 100 uncoded QPSK modulated symbols are simulated per VC per channel realization. The SER curves are obtained by averaging over 10^5 channel realizations. The average total transmit power is held at 1, and the noise variance is adjusted to reflect the signal-to-noise ratio (SNR).

A. Application in Two-User MIMO Multicasting

Consider a simple two-user MIMO broadcast/multicast configuration (see Fig. 1) that corresponds to a source $\mathcal{S}$ that caters to the users $\mathcal{U}_1$ and $\mathcal{U}_2$. Being the simplest possible GSVD beamforming application, this system is ideal for investigating the PC/CC performance and the effect of channel-estimation errors and channel fading on it.

Fig. 4(a)–(d) depicts the SER curves for the following antenna configurations, and it is assumed that i.i.d. Rayleigh fading affects both users.

- Fig. 4(a) corresponds to the $(N, M_1, M_2) \doteq (4, 2, 2)$ configuration, where the source has four spatial DoFs, i.e., just as many as the two users' combined. As speculated in Section III, GSVD beamforming yields identical PCs as with transmit ZF. (In the other three cases, corresponding to Fig. 4(b)–(d), the source does not have sufficient antennas to perform ZF.)
- Fig. 4(b) corresponds to the $(N, M_1, M_2) \doteq (4, 3, 2)$ scenario. The single CC utilizes one of the DoFs at the source; the remaining DoFs facilitate the PCs. Clearly, this CC and PC allocation yields the highest multiplexing gain, as is always the case with GSVD beamforming. As speculated in Section II, the PCs show identical SER performance, whereas the CCs perform worse. Notably, the two users experience different SER performance with respect to the same CC. This observation indicates that coding techniques for the single-antenna broadcast channel [25] can be employed to exploit the capacity of a CC.
- The $(N, M_1, M_2) \doteq (4, 3, 3)$ antenna configuration, whose SER performance is shown in Fig. 4(c), is even more interesting, because each of the two CCs imparts different SERs upon its end users. Statistical symmetry in the $\mathcal{S} \rightarrow \mathcal{U}_1$ and $\mathcal{S} \rightarrow \mathcal{U}_2$ MIMO channels (i.e., $M_1 = M_2$ and the channels being i.i.d. Rayleigh fading) makes the SER experienced by $\mathcal{U}_1$ for CC$_1$ identical to that experienced by $\mathcal{U}_2$ for CC$_2$. Similar observations can be made with regard to $\mathcal{U}_2$'s experience for CC$_1$ and $\mathcal{U}_1$'s for CC$_2$. The SER degrades from CC$_1$ to CC$_2$ for $\mathcal{U}_1$, whereas it improves for $\mathcal{U}_2$; this observation is consistent with the fact that, in GSVD, the coefficients α_i's appear in descending order, whereas the $\beta_i = \sqrt{1 - \alpha_i^2}$, $i \in \{1, \ldots, s\}$ ascend.
- Fig. 4(d) corresponds to the case $N = M_1 = M_2 = 4$. GSVD beamforming yields four CCs. The symmetry dictates that the SER performance for $\mathcal{U}_1$'s CC$_k$ is identical to that of $\mathcal{U}_2$'s CC$_{(5-k)}$ for $k \in \{1, \ldots, 4\}$. Again, for $\mathcal{U}_1$, the performance degrades from CC$_1$ to CC$_4$.

Note that the SER curves exhibit no error floors; i.e., interchannel interference is perfectly eliminated for both users.

Fig. 4(a)–(d) assumes the availability of perfect CSI. What would happen with imperfect CSI? Fig. 5 shows the effect of channel-estimation errors on the SER if we consider CC$_1$ of $\mathcal{U}_1$ in the $(N, M_1, M_2) \doteq (3, 2, 2)$ configuration and assume i.i.d. Rayleigh fading. For each channel matrix $\mathbf{H}_i$, $i \in \{1, 2\}$, the channel-estimation error $\sigma\mathbf{\Delta H}_i$ is assumed to be complex Gaussian with zero mean and σ^2 variance, and the channel estimate $\hat{\mathbf{H}}_i = \mathbf{H}_i + \sigma\mathbf{\Delta H_i}$ is used for computing
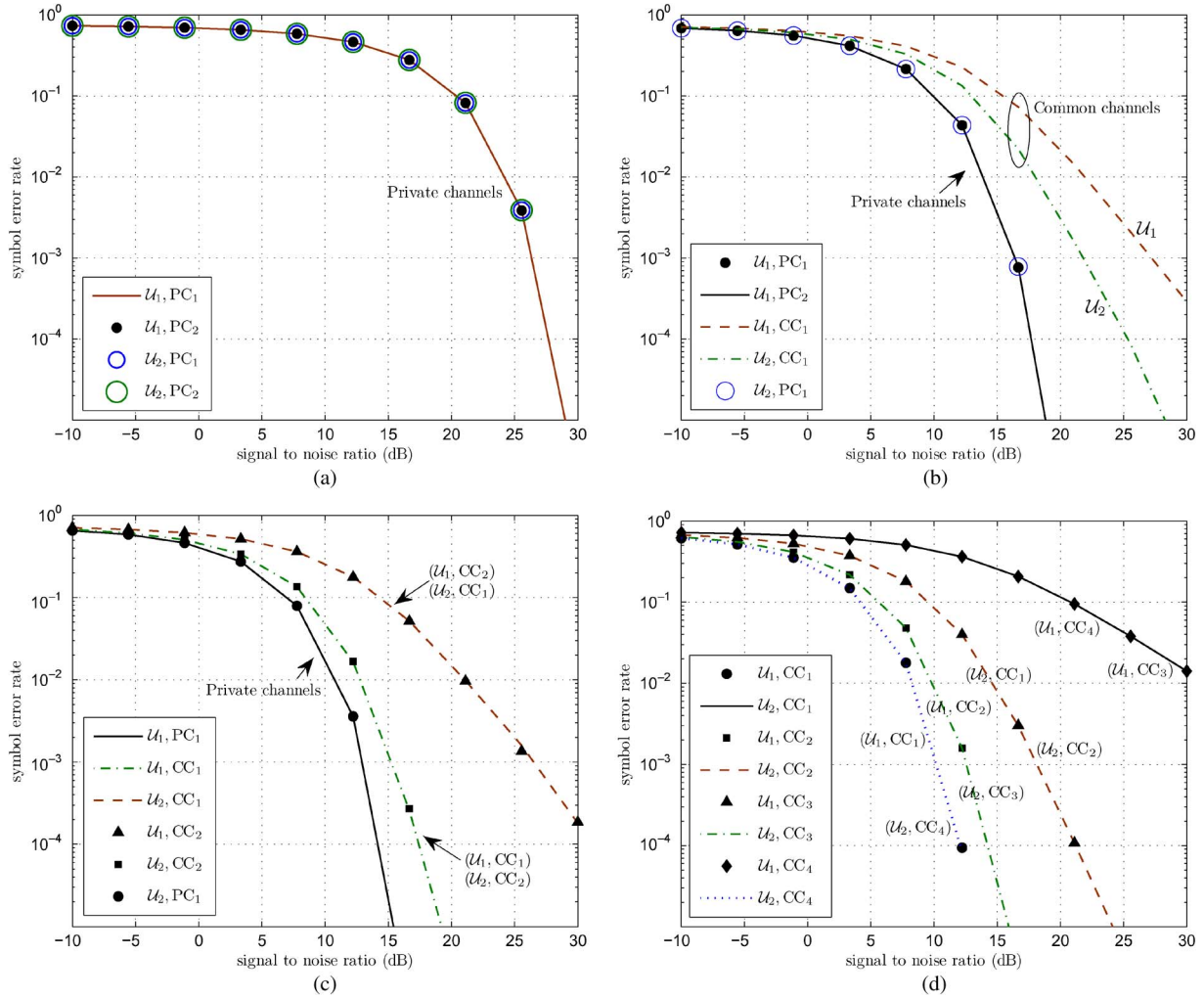
Fig. 4. SERs of the PCs and CCs in (N, M_1, M_2)-antenna two-user multicast configurations. QPSK modulation is used. (a) $(N, M_1, M_2) \doteq (4, 2, 2)$. (b) $(N, M_1, M_2) \doteq (4, 3, 2)$. (c) $(N, M_1, M_2) \doteq (4, 3, 3)$. (d) $(N, M_1, M_2) \doteq (4, 4, 4)$.
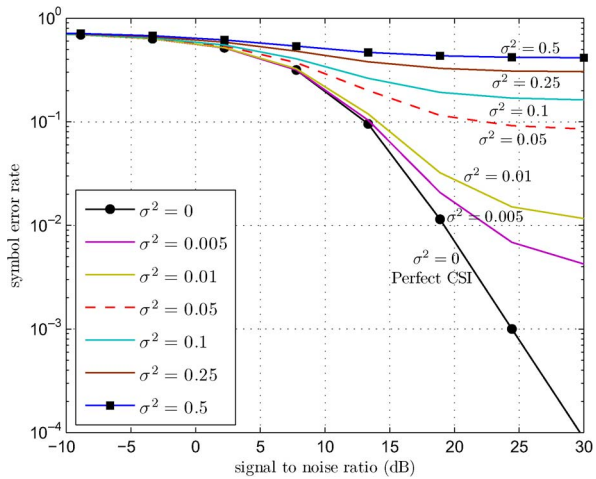

Fig. 5. SER of CC$_1$ for $\mathcal{U}_1$ subject to imperfect CSI in the $(N, M_1, M_2) \doteq (3, 2, 2)$ two-user multicast configuration. QPSK modulation and complex Gaussian channel-estimation errors with σ^2 variance are assumed.

the beamforming matrices. As expected, with increasing σ^2, the performance rapidly degrades, producing error floors. For example, a 10-dB degradation occurs for $\sigma^2 = 0.01$, even at the relatively high 10^{-2} SER level. Such degradation should

be expected, given the presence of multiple spatially separated VCs; however, it emphasizes the crucial role of channel estimation with GSVD beamforming.

Fig. 6(a) and (b) shows the SER performance for asymmetric configurations, in which $\mathcal{U}_1$ experiences, on the average, a 3-dB stronger channel compared with $\mathcal{U}_2$. Rayleigh fading is also assumed here. As with Fig. 4(a), GSVD beamforming produces four identical PCs for the case depicted in Fig. 6(a). The relative merits of the SER curves in Fig. 6(b), however, differ from the corresponding symmetric case depicted in Fig. 4(c); because $\mathcal{U}_1$ has a stronger channel, the symmetry observable in Fig. 4(c) no longer holds for Fig. 6(b). Even here, the PCs deliver the best error rates, as expected.

The MIMO channels that correspond to Fig. 7 are asymmetric, because only $\mathcal{U}_1$'s channel has a specular component. More specifically, the $\mathcal{S} \rightarrow \mathcal{U}_1$ channel undergoes Rician fading, with a Rice factor of 1 and a nonentrality matrix having (arbitrarily chosen) eigenvalues $\{8.83, 2.39\}$; the $\mathcal{S} \rightarrow \mathcal{U}_2$ channel undergoes i.i.d. Rayleigh fading that is statistically identical to the scatter component of the $\mathcal{S} \rightarrow \mathcal{U}_1$. The symmetry observed in Fig. 4(c) with respect to the CC SER performance is no longer present in this scenario. The line-of-sight component of $\mathcal{S} \rightarrow \mathcal{U}_1$ channel is seen to improve the SER $\mathcal{U}_1$ experiences for the
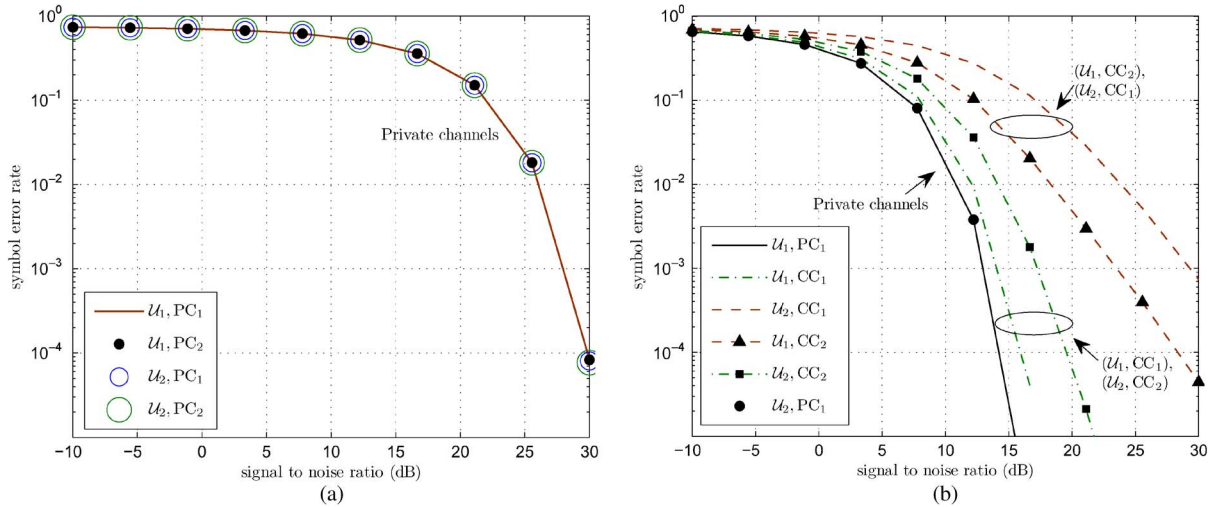
Fig. 6. SERs of the PCs and CCs in (N, M_1, M_2)-antenna asymmetric two-user multicast configurations. The $\mathcal{S} \to \mathcal{U}_1$ channel is 3 dB stronger than the $\mathcal{S} \to \mathcal{U}_2$ channel. QPSK modulation is used. (a) $(N, M_1, M_2) \doteq (4, 2, 2)$. (b) $(N, M_1, M_2) \doteq (4, 3, 3)$.

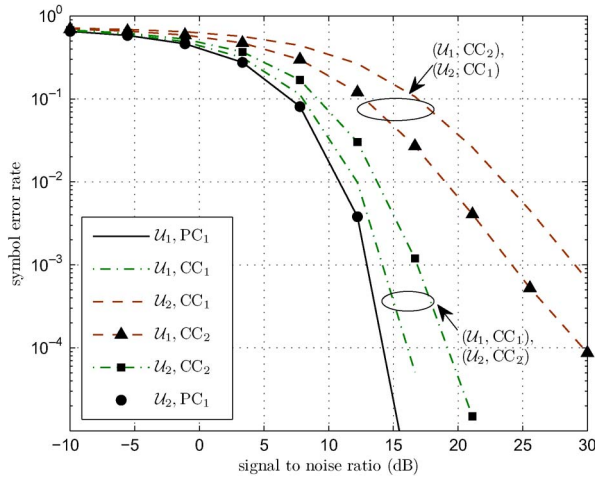Fig. 7. SRs of the PCs and CCs in the $(N, M_1, M_2) \doteq (4, 3, 3)$ two-user multicast configuration under asymmetric fading. The $\mathcal{S} \to \mathcal{U}_1$ and $\mathcal{S} \to \mathcal{U}_2$ channels undergo Rician fading and Rayleigh fading, respectively. QPSK modulation is used.

Fig. 8. Network-coded MIMO two-way relay system.

CCs. Nevertheless, the SER performance of the PCs is identical for both users, confirming that GSVD, irrespective of the fading distribution, yields PCs with an identical (and constant) gain.

B. Application in Network-Coded Two-Way Relaying

In this section, the SER performance of two-way relaying (see Fig. 8) with physical-layer network coding [26] is investigated.

The channelization scheme involves two time slots that correspond to uplink and downlink transmissions, respectively. In the uplink, the users simultaneously transmit precoded data; the relay jointly decodes the received signal (by using the corresponding superimposed constellation) such that the transmitted data effectively "XOR in the air" [27], and the XOR operation is manifested as physical-layer network coding. In the downlink time slot, the relay regenerates the decoded data (which are now the XOR of the two users' data, possibly with noise-introduced errors) and broadcasts to both users; each user may extract the other user's data by detecting the
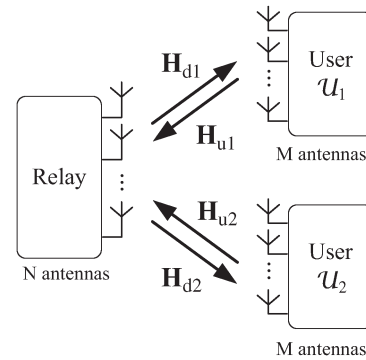
received signal and performing an XOR operation away its own (transmitted) data.

Suppose that the relay has N antennas and that each user $\mathcal{U}_i$, $i \in \{1, 2\}$ has M antennas; N VCs, VC_i for $i \in \{1, \ldots, N\}$, are to be realized in each direction $\mathcal{U}_1 \to \mathcal{U}_2$ and $\mathcal{U}_2 \to \mathcal{U}_1$ through the relay. A constraint $N < M$ is imposed to make ZF transmission/reception realizable at the users; it also ensures that GSVD beamforming yields only CCs, as physical-layer network coding requires. Let $\mathbf{H}_{u1}$, $\mathbf{H}_{u2} \in \mathbb{C}^{N \times M}$ denote the uplink MIMO channels from $\mathcal{U}_1$ and $\mathcal{U}_2$, respectively; $\mathbf{H}_{d1}$, $\mathbf{H}_{d2} \in \mathbb{C}^{M \times N}$ are the corresponding downlink MIMO channels from the relay. If time-division duplexing is used, $\mathbf{H}_{d1} = \mathbf{H}_{u1}^T$ and $\mathbf{H}_{d2} = \mathbf{H}_{u2}^T$ hold due to channel reciprocity.

Consider the following three channelization schemes.

- *Scheme 1*: ZF transmission is used in the uplink, whereas GSVD beamforming is used in the downlink.
- *Scheme 2*: ZF transmission and reception are employed, respectively, in the uplink and the downlink.
- *Scheme 3*: GSVD beamforming is used in the downlink, whereas a multiple-access variant of GSVD beamforming implements the uplink.

Scheme 1: Here, transmit ZF is employed in the uplink. Thus, the transmit beamforming matrices at $\mathcal{U}_1$ and $\mathcal{U}_2$ are $\mathbf{W}_1 = \alpha_u (\mathbf{H}_{u1})^\dagger$ and $\mathbf{W}_2 = \alpha_u (\mathbf{H}_{u2})^\dagger$, respectively. Receiver beamforming at the relay, represented by a matrix $\mathbf{R} = \mathbf{I}_N / \alpha_u$,

merely involves normalization; α_u is the transmit power normalization coefficient.

Because the downlink is a two-user broadcast channel, GSVD beamforming can be applied unmodified on $\mathbf{H}_{d1}$ and $\mathbf{H}_{d2}$. Let $\mathbf{H}_{d1} = \mathbf{U}_{d1}\boldsymbol{\Sigma}_{d1}\mathbf{V}_d$ and $\mathbf{H}_{d2} = \mathbf{U}_{d2}\boldsymbol{\Sigma}_{d2}\mathbf{V}_d$ be the corresponding GSVD, where $\mathbf{V}_d \in \mathbb{C}^{N \times N}$ represents the common factor given by the decomposition, i.e., the factor $(\mathbf{W}^H\mathbf{R}, \mathbf{0})\mathbf{Q}^H$ in (2).

The following choice of transmit beamforming matrix $\mathbf{W}$ (for the relay) and the receiver beamforming matrices $\mathbf{R}_1, \mathbf{R}_2$ (for $\mathcal{U}_1$ and $\mathcal{U}_2$, respectively) ensures joint diagonalization of the MIMO channels:

$$\mathbf{W} = \alpha_d \cdot (\mathbf{V}_d)^{-1} \tag{10a}$$

$$\mathbf{R}_1 = \frac{1}{\alpha_d} \cdot \left\{\mathbf{U}_{d1}^H\right\}_{\mathcal{R}(1:N)} \tag{10b}$$

$$\mathbf{R}_2 = \frac{1}{\alpha_d} \cdot \left\{\mathbf{U}_{d2}^H\right\}_{\mathcal{R}(M-N+1:M)}. \tag{10c}$$

The corresponding VC gains for $\mathcal{U}_1$ and $\mathcal{U}_2$ are, respectively, given by $\operatorname{diag}(\{\boldsymbol{\Sigma}_{d1}\}_{\mathcal{R}(1:N)})$ and $\operatorname{diag}(\{\boldsymbol{\Sigma}_{d2}\}_{\mathcal{R}(M-N+1:N)})$; α_d normalizes the average relay transmit power.

Scheme 2: In this scheme, beamforming for the uplink is the same as in Scheme 1. However, ZF reception is employed in the downlink. Thus, the corresponding beamforming matrices are $\mathbf{W}_1 = \beta_u(\mathbf{H}_{u1})^\dagger$, $\mathbf{W}_2 = \beta_u(\mathbf{H}_{u2})^\dagger$, $\mathbf{R} = \mathbf{I}_N/\beta_u$, $\mathbf{W} = \beta_d\mathbf{I}_N$, $\mathbf{R}_1 = (\mathbf{H}_{d1})^\dagger/\beta_d$, and $\mathbf{R}_2 = (\mathbf{H}_{d2})^\dagger/\beta_d$, where β_u and β_d, respectively, normalize the average transmit power in the uplink and downlink time slots. Note that $\mathcal{U}_1$ and $\mathcal{U}_2$ are responsible for all the MIMO signal processing in both directions.

Scheme 3: Here, GSVD beamforming is employed in the reverse direction for the uplink, with a minor modification to ensure that the effective CC gains are 1. Consider the GSVD of $\mathbf{H}_{u1}^T \in \mathbb{C}^{M \times N}$ and $\mathbf{H}_{u2}^T \in \mathbb{C}^{M \times N}$ given by $\mathbf{H}_{u1}^T = \mathbf{U}_{u1}\boldsymbol{\Sigma}_{u1}\mathbf{V}_u$ and $\mathbf{H}_{u2}^T = \mathbf{U}_{u2}\boldsymbol{\Sigma}_{u2}\mathbf{V}_u$. The transmit beamforming matrices

$$\begin{aligned}\mathbf{W}_1 &= \delta_u \cdot \left((\mathbf{U}_{u1}\boldsymbol{\Sigma}_{u1})^\dagger\right)^T \\ &= \delta_u \cdot \left(\{\mathbf{U}_{u1}\}_{\mathcal{C}(1:N)}\right)^* \cdot \left(\{\boldsymbol{\Sigma}_{u1}\}_{\mathcal{R}(1:N)}\right)^{-1} \text{ and} \end{aligned} \tag{11a}$$

$$\begin{aligned}\mathbf{W}_2 &= \delta_u \cdot \left((\mathbf{U}_{u2}\boldsymbol{\Sigma}_{u2})^\dagger\right)^T \\ &= \delta_u \cdot \left(\{\mathbf{U}_{u2}\}_{\mathcal{C}(M-N+1:M)}\right)^* \\ &\quad \cdot \left(\{\boldsymbol{\Sigma}_{u2}\}_{\mathcal{R}(M-N+1:M)}\right)^{-1} \end{aligned} \tag{11b}$$

respectively, for $\mathcal{U}_1$ and $\mathcal{U}_2$ and the receiver beamforming matrix

$$\mathbf{R} = \frac{1}{\delta_u} \cdot (\mathbf{V}_u^{-1})^T \tag{11c}$$

for the relay jointly force each effective uplink channel to be a rank-N identity matrix. δ_u normalizes the average total user transmit power. The transmitter–receiver processing involved here can thus be interpreted as a form of simultaneous transmit and receiver ZF. Downlink beamforming is the same as with Scheme 1; therefore, $\mathbf{W}$, $\mathbf{R}_1$, and $\mathbf{R}_2$ are given by equations similar to (10a)–(10c).

Fig. 9 compares the SER performance of the aforementioned three schemes for a MIMO two-way relay system with $(M, N) \doteq (4, 3)$.
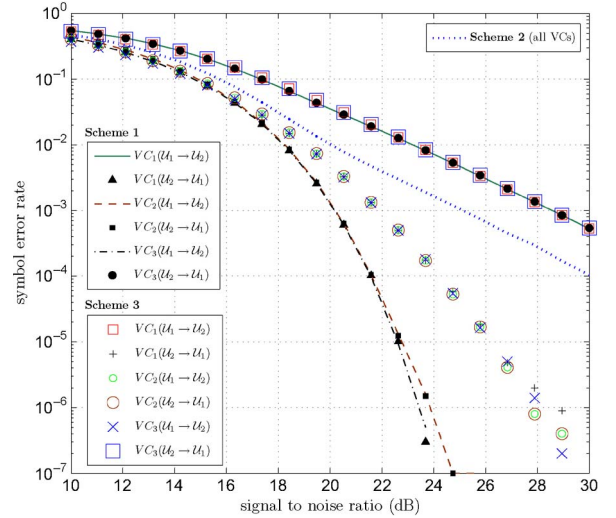

Fig. 9. SERs of the VCs in the $(M, N) \doteq (4, 3)$ network-coded MIMO two-way relay configuration. QPSK modulation is used.

Assumptions: QPSK modulation with binary symbol mapping is assumed at $\mathcal{U}_1$ and $\mathcal{U}_2$. The relay directly decodes the XORed symbols by using the maximum-likelihood detection rule on the corresponding superimposed constellation and remodulates the regenerated symbols by using QPSK. Time-division duplexing, channel reciprocity, and symmetric two-way relay configuration undergoing i.i.d. Rayleigh fading are assumed. Normalization coefficients are selected to cause the average transmit power used by each user, and the relay is 1/3 power unit. Each scheme produces three VCs in either direction as follows.

- *Scheme* 1. Except for the weakest VC in each direction (i.e., VC$_1$ in the $\mathcal{U}_1 \to \mathcal{U}_2$ direction and VC$_3$ in the $\mathcal{U}_2 \to \mathcal{U}_1$ direction) having a diversity order of 2, all other VCs exhibit the same SER performance, faring better than the VCs produced by scheme 2. (The weakest VCs are about 4 dB worse than those.)
- *Scheme* 2. All the VCs exhibit the same SER performance and a diversity order of 2, faring worse than all but the weakest VCs of schemes 1 and 3.
- *Scheme* 3. The weakest VCs are exactly those of scheme 1 and exhibit the same SER as they do. All the other VCs perform identically but have the SERs between schemes 1 and 3.

To summarize, scheme 1 fares impressively compared to scheme 2, which is the transmit and receiver ZF-based MIMO two-way relay network implementation typically considered in the literature. In addition, GSVD beamforming appears to perform the best, when employed in the downlink, in its original form.

With physical-layer network coding, the overall SER that corresponds to each VC is approximately the worst SER that it experiences in either of the hops: the uplink or the downlink. Therefore, the aforementioned observations can be explained by using a hop-by-hop SER analysis. Given the lack of exact analytical results, we resort to intuitions and simulation results (see Fig. 10) for this purpose. Because the two-way relay configuration concerned is symmetric, it is sufficient to consider a single direction (e.g., the $\mathcal{U}_1 \to \mathcal{U}_2$ direction through the relay).
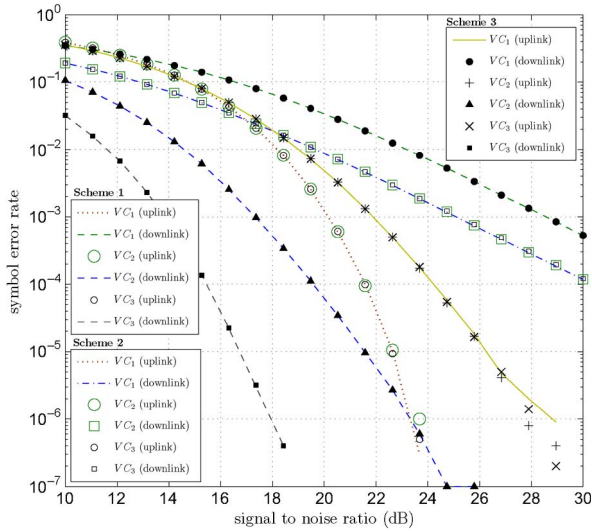
Fig. 10. Hop-by-hop SERs of the VCs (for the $\mathcal{U}_1 \rightarrow \mathcal{U}_2$ direction) in the $(M, N) \doteq (4, 3)$ network-coded MIMO two-way relay configuration. QPSK modulation is used.

Because no preordering of the VCs happens at the transmitter, for a given scheme, all the VCs experience the same SER in the uplink. Therefore, the performance distinctions among the VCs realized by a given scheme can be attributed to downlink beamforming. According to Theorem 1, GSVD beamforming in the downlink causes each VC_r in the $\mathcal{U}_2 \rightarrow \mathcal{U}_1$ direction and each $VC_{(N-r+1)}$ in the $\mathcal{U}_1 \rightarrow \mathcal{U}_2$ direction to have a diversity order $(M - r + 1)(N - r + 1)$ for $r \in \{1, \ldots, N\}$. Therefore, the weakest VC has a diversity order $(M - N + 1)$ similar to that of a ZF-based downlink. Confirming these facts, the downlink VC_1 and VC_2 for schemes 1 and 3 are observed (see Fig. 10) to have diversity orders of 2 and 6, respectively. (Low Monte Carlo precision precludes curves that correspond to VC_3 from showing a diversity order of 12.) Moreover, the downlink VCs for scheme 2 show a diversity order of 2. Despite having the same diversity order, ZF reception can be observed to yield better SER than that of the weakest VC realized through GSVD beamforming. These performance distinctions are manifested in the overall SER of a VC (see Fig. 9) whenever its uplink SER is better than the downlink SER.

Transmit ZF makes the uplink effectively additive Gaussian, potentially yielding infinite diversity orders. However, as evident in Fig. 10, the corresponding SER is worse than all but the weakest VC of a GSVD downlink (even at the 10^{-5} SER level). As a result, for scheme 1, the downlink governs the overall SER of the weakest VC, whereas the uplink appears to dictate those of all other VCs. However, at even higher SNR values (and impractically low SER levels), the downlink would dominate the performance of all the VCs. Thus, theoretically, the diversity orders of scheme 1 will be those of a GSVD downlink (with each VC performing differently). For scheme 2, the downlink dictates the overall SER, except at low-SNR values. Thus, the SER performance of schemes 1 and 3 observed in Fig. 9 may qualitatively be explained by using the worst of uplink and downlink SERs. The performance of scheme 3 may similarly be explained. Moreover, because GSVD uplink beamforming does not completely negate fading as transmit ZF does, GSVD uplink VCs perform worse than their transmit ZF counterparts.

This fact, which is also observed in Fig. 10, explains the relative performance difference in schemes 1 and 3.

VII. Conclusion

This paper has investigated GSVD beamforming, a noniterative two-user beamforming technique that was proposed in [10] and produces point-to-two-point (common) VCs in addition to the classic point-to-point (private) VCs. The dependency of the numbers of PCs/CCs on the channel ranks and transmit power normalization was investigated. Moreover, the joint pdf of channel gains was derived for Rayleigh fading and MIMO configurations that support only CCs. Corresponding diversity orders were derived based on this pdf result, and they are the first exact analytical result on GSVD beamforming. Moreover, through the SER simulation of elementary multicasting and two-way relaying applications, the performance distinctions of the PCs/CCs and the effect of channel-estimation errors and asymmetries in channel fading were highlighted.

Future directions related to this research are as follows.

- As illustrated in Theorem 1, the framework based on Proposition 1 can be used to quantify the performance of certain GSVD beamforming configurations. Obtaining such numerical (and, perhaps, exact analytical) performance results are among future possibilities. Generalizing Proposition 1 to eliminate the condition $\min(m, p) \geq k$ is a more challenging possibility; such generalization would also contribute to a random matrix theory.
- The capacity of the two-user MIMO downlink and the SER under GSVD beamforming would be useful for determining how GSVD beamforming ranks compared to the other channelization schemes. For example, generalized eigenvector-based techniques (e.g., [16] and [17]) may be employed in all but certain rank-deficient channels that GSVD beamforming supports. Therefore, performance comparison with generalized eigenvector-based techniques is important to assess the usefulness of GSVD beamforming.
- GSVD beamforming assumes perfect CSI; developing "robust" counterparts that achieve acceptable SER performance under imperfect CSI has a greater practical significance.

Appendix
Proof of Theorem 1: Diversity Order

Proof: Consider GSVD beamforming over MIMO channels $\mathbf{H}_1 \in \mathbb{C}^{m \times n}$ and $\mathbf{H}_2 \in \mathbb{C}^{p \times n}$ undergoing i.i.d. Rayleigh fading, corresponding to users $\mathcal{U}_1$ and $\mathcal{U}_2$, respectively. Suppose rank $((\mathbf{H}_1^H \mathbf{H}_2^H)) = k \leq \min(m, p)$.

The variable transformation $\gamma_i = \alpha_i^2, i \in \{1, \ldots, k\}$ on (4) gives the ordered joint pdf $f_\gamma(\gamma_1, \ldots, \gamma_k)$ as

$$f_\gamma(\gamma_1, \ldots, \gamma_k) \propto \prod_{i=1}^{k} \gamma_i^{m-k}(1 - \gamma_i)^{p-k}$$
$$\times \prod_{1 \leq i < j \leq k} (\gamma_i - \gamma_j)^2 \quad (12)$$

for $1 \geq \gamma_1 \geq \gamma_2 \geq \ldots \geq \gamma_k \geq 0$.

Integrating out γ_i, $i \neq r$ of (12), yields the following marginal pdf of γ_r:

$$f_{\gamma_r}(\gamma_r) \propto \underbrace{\int_{\gamma_{r+1}=0}^{\gamma_r} \int_{\gamma_{r+2}=0}^{\gamma_{r+1}} \dots \int_{\gamma_{k=0}}^{\gamma_{k-1}}}_{(k-r) \text{ cascaded integrations}}$$

$$\times \underbrace{\int_{\gamma_{r-1}=\gamma_r}^{1} \int_{\gamma_{r-2}=\gamma_{r-1}}^{1} \dots \int_{\gamma_1=\gamma_2}^{1}}_{(r-1) \text{ cascaded integrations}}$$

$$\times f_\gamma(\gamma_1, \dots, \gamma_k) \mathrm{d}_{\gamma_1} \dots \mathrm{d}_{\gamma_{r-1}} \mathrm{d}_{\gamma_{r+1}} \dots \mathrm{d}_{\gamma_k}. \tag{13}$$

Note that $f_{\gamma_r}(\gamma_r)$ will be a polynomial of γ_r alone and that we are interested only in its *least order term*.

The joint pdf (12) is a homogeneous multivariate polynomial of γ_i's, and given any of its terms, integration by each γ_i raises the corresponding degree by 1. Because each of the $(k-r)$ cascaded integrations that involve γ_i, $i > r$ has 0 as the lower limit of integration and γ_{i-1} as the upper limit, each integration increases the degree of γ_r in the resulting expression by one. As a result, the degree of the least order term of $f_{\gamma_r}(\gamma_r)$ is incremented by $(k-r)$. By contrast, having a nonzero constant of 1 as the upper limit of integration, none of the $(r-1)$ remaining cascaded integrals (corresponding to γ_i, $i < r$) has any effect on the degree of γ_r in the desired least order term. Thus, we need to consider only the powers of γ_i, $i \geq r$ in the integrand for diversity-order analysis.

In addition, for our purpose

$$\prod_{i=1}^{k} \gamma_i^{m-k}(1-\gamma_i)^{p-k} = \prod_{i=r}^{k} \gamma_i^{m-k} + \text{higher order terms} \tag{14}$$

which contributes $(m-k)(k-r+1)$ degrees to the least order term. The sum of degrees of γ_i, $i \geq r$ in the factor $\Pi_{1 \leq i < j \leq k}(\gamma_i - \gamma_j)^2$ in (12) is minimal in its term that corresponds to $\Pi_{i=1}^{k-1}\gamma_i^{2(k-i)}$. This term yields $2\Sigma_{i=r}^{k-1}(k-i) = (k-r)(k-r+1)$ degrees toward the diversity order.

Thus, the degree of γ_r in the least order term of $f_{\gamma_r}(\gamma_r)$ comes to

$$n_r = (m-k)(k-r+1) + (k-r)(k-r+1) + (k-r) \tag{15a}$$

$$= (m-r+1)(k-r+1) - 1. \tag{15b}$$

The term $(k-r)$ in (15a) represents the increment due to the $(k-r)$ cascaded integrations.

Based on (15b) and by using [28], we get the diversity order of the rth CC for user $\mathcal{U}_1$ to be $n_r + 1 = (m-r+1)(k-r+1)$ for $r \in \{1, \dots, k\}$, completing the proof. ∎

REFERENCES

[1] *IEEE Standard for Information Technology—Telecommunications and Information Exchange Between Systems Local and Metropolitan Area Networks-Specific Requirements Part 11: Wireless LAN Medium Access Control (MAC) and Physical Layer (PHY) Specifications*, IEEE Std. 802.11, Mar. 2012.

[2] *Technical Specification Group Radio Access Network: Evolved Universal Terrestrial Radio Access (E-UTRA) and Evolved Universal Terrestrial Radio Access Network (E-UTRAN-): Overall Description Stage 2 (Rel. 10)*, Third-Generation Partnership Project TS 36.300 V10, Jun. 2010.

[3] Q. H. Spencer, A. L. Swindlehurst, and M. Haardt, "Zero-forcing methods for downlink spatial multiplexing in multiuser MIMO channels," *IEEE Trans. Signal Process.*, vol. 52, no. 2, pp. 461–471, Feb. 2004.

[4] N. D. Sidiropoulos, T. N. Davidson, and Z.-Q. Luo, "Transmit beamforming for physical-layer multicasting," *IEEE Trans. Signal Process.*, vol. 54, no. 6, pp. 2239–2251, Jun. 2006.

[5] S. Shi, M. Schubert, and H. Boche, "Physical-layer multicasting with linear MIMO transceivers," in *Proc. CISS*, Princeton, NJ, USA, Mar. 2008, pp. 884–889.

[6] I. H. Kim, D. J. Love, and S. Y. Park, "Recursive covariance design for multiple-antenna physical-layer multicasting," in *Proc. IEEE Radio Wireless Symp.*, Orlando, FL, USA, Jan. 2008, pp. 555–558.

[7] J. Li and A. P. Petropulu, "On transmit beamforming for physical-layer multicasting," in *Proc. IEEE GLOBECOM*, Houston, TX, USA, Dec. 2011, pp. 1–5.

[8] M. A. Khojastepour, A. Salehi-Golsefidi, and S. Rangarajan, "Towards an optimal beamforming algorithm for physical-layer multicasting," in *Proc. IEEE ITW*, Paraty, Brazil, Oct. 2011, pp. 395–399.

[9] I. H. Kim, D. J. Love, and S. Y. Park, "Optimal and successive approaches to signal design for multiple-antenna physical-layer multicasting," *IEEE Trans. Commun.*, vol. 59, no. 8, pp. 2316–2327, Aug. 2011.

[10] D. Senaratne and C. Tellambura, "Generalized singular value decomposition for coordinated beamforming in MIMO systems," in *Proc. IEEE GLOBECOM*, Miami, FL, USA, Dec. 2010.

[11] C. F. V. Loan, "Generalizing the singular value decomposition," *SIAM J. Numer. Anal.*, vol. 13, no. 1, pp. 76–83, Mar. 1976.

[12] G. Strang, *Linear Algebra and Its Applications*, 2nd ed. Orlando, FL, USA: Academic, 1980.

[13] A. Khisti, G. Wornell, A. Wiesel, and Y. Eldar, "On the Gaussian MIMO wiretap channel," in *Proc. IEEE ISIT*, Nice, France, Jun. 2007, pp. 2471–2475.

[14] S. A. A. Fakoorian and A. L. Swindlehurst, "Optimal power allocation for GSVD-based beamforming in the MIMO Gaussian wiretap channel," in *Proc. IEEE ISIT*, Cambridge, MA, USA, Jul. 2012, pp. 2321–2325.

[15] Y. Fu, L. Yang, and Z. He, "Amplify-and-forward relaying scheme based on GSVD for MIMO relay networks," in *Proc. ICNNSP*, Nanjing, China, Jun. 2008, pp. 506–511.

[16] C.-B. Chae, D. Mazzarese, N. Jindal, and R. Heath, "Coordinated beamforming with limited feedback in the MIMO broadcast channel," *IEEE J. Sel. Areas Commun.*, vol. 26, no. 8, pp. 1505–1515, Oct. 2008.

[17] K.-H. Park, Y.-C. Ko, and M.-S. Alouini, "Low-complexity noniterative coordinated beamforming in two-user broadcast channels," *IEEE Trans. Commun.*, vol. 58, no. 10, pp. 2810–2815, Oct. 2010.

[18] C. C. Paige and M. A. Saunders, "Towards a generalized singular value decomposition," *SIAM J. Numer. Anal.*, vol. 18, no. 3, pp. 398–405, Jun. 1981.

[19] A. M. Tulino and S. Verdu, *Random Matrix Theory and Wireless Communications*, 1st ed. Hanover, MA, USA: Now, 2004, ser. Foundations and Trends in Communications and Information Theory.

[20] K. Zyczkowski and H.-J. Sommers, "Truncations of random unitary matrices," *J. Phys. A, Math. Gen.*, vol. 33, no. 10, pp. 2045–2057, Mar. 2000.

[21] P. J. Forrester and M. Krishnapur, "Derivation of an eigenvalue probability density function relating to the Poincaré disk," *J. Phys. A: Math. Theor.*, vol. 42, no. 38, pp. 385204-1–385204-10, Sep. 2009.

[22] B. D. Sutton, "The stochastic operator approach to random matrix theory," Ph.D. dissertation, Dept. Math., Mass. Inst. Technol., Cambridge, MA, USA, 2005.

[23] A. Edelman and B. D. Sutton, "The beta-Jacobi matrix model, the CS decomposition, and generalized singular value problems," *Found. Comput. Math.*, vol. 8, no. 2, pp. 259–285, May 2008.

[24] I. Dumitriu and A. Edelman, "Matrix models for beta ensembles," *J. Math. Phys.*, vol. 43, no. 11, pp. 5830–5847, Nov. 2002.

[25] T. Cover, "Broadcast channels," *IEEE Trans. Inf. Theory*, vol. IT-18, no. 1, pp. 2–14, Jan. 1972.

[26] P. Popovski and H. Yomo, "Physical network coding in two-way wireless relay channels," in *Proc. IEEE ICC*, Glasgow, U.K., Jun. 2007, pp. 707–712.

[27] S. Katti, H. Rahul, W. Hu, D. Katabi, M. Médard, and J. Crowcroft, "XORs in the air: Practical wireless network coding," in *Proc. ACM SIGCOMM*, Pisa, Italy, Sep. 2006, pp. 243–254.

[28] Z. Wang and G. Giannakis, "A simple and general parameterization quantifying performance in fading channels," *IEEE Trans. Commun.*, vol. 51, no. 8, pp. 1389–1398, Aug. 2003.

Damith Senaratne (M'13) received the B.Sc. degree in electronic and telecommunication engineering and the M.Sc. degree in telecommunications from the University of Moratuwa, Katubedda, Sri Lanka, in 2005 and 2008, respectively, and the Ph.D. degree in communications from the University of Alberta, Edmonton, AB, Canada, in 2012.

He is currently a Research Assistant with the Department of Electrical and Computer Engineering, University of Alberta. His research interests include multiple-input–multiple-output signal processing, multicarrier transmission, and fading countermeasures.

Chintha Tellambura (F'11) received the Ph.D. degree in electrical engineering from the University of Victoria, Victoria, BC, Canada, in 1993.

He was a Postdoctoral Research Fellow with the University of Victoria from 1993 to 1994 and with the University of Bradford, Bradford, U.K., from 1995 to 1996. From 1997 to 2002, he was with Monash University, Clayton, Vic., Australia. He is currently a Professor with the Department of Electrical and Computer Engineering, University of Alberta, Edmonton, AB, Canada. His research interests include wireless physical-layer issues, multiple-antenna systems, orthogonal frequency-division multiplexing, relay networks, cognitive radio, and interference in wireless networks.

Prof. Tellambura was an Associate Editor for the IEEE TRANSACTIONS ON COMMUNICATIONS and the Area Editor for Wireless Communications Systems and Theory for the IEEE TRANSACTIONS ON WIRELESS COMMUNICATIONS (TWC). He is currently an Editorial Advisory Board Member of the TWC. He was the Chair of the Communication Theory Symposium at the 2005 IEEE Global Telecommunications Conference. He received the Killam Professor Award and the McCalla Professor Award from the University of Alberta and the Communication Theory Best Paper Award at the 2012 IEEE International Conference on Communications.